Supporting Information for:

Nanofibers generated from nonclassical organogelators based on difluoroboron β-diketonate complexes to detect aliphatic primary amine vapors

Lu Zhai, Mingyang Liu, Pengchong Xue, Jingbo Sun, Peng Gong, Zhenqi Zhang, Jiabao Sun and Ran Lu*

State Key Laboratory of Supramolecular Structure and Materials, College of Chemistry, Jilin University, Changchun 130012, P. R. China

E-mail: luran@mail.jlu.edu.cn

Contents:

Table S1. Photophysical data of **ABA**, **ABVA** and **AVBVA**.

Complex	Solvent	λ_{abs} (nm)	λ_{em} (nm)	Stokes shift (cm^{-1})	Φ_F[a]
ABA	Cyclohexane	488	518	1186	-
	Toluene	500	552	1884	0.97
	THF	501	585	2866	0.21
	Acetone	502	612	3580	-
	DMSO	516	614	3093	-
ABVA	Cyclohexane	501, 527	553	892	-
	Toluene	541	590	1535	0.70
	THF	539	632	2729	0.15
	Acetone	542	655	3183	-
	DMSO	560	678	3108	-
AVBVA	Cyclohexane	525, 558	582	739	-
	Toluene	574	621	1319	0.82
	THF	573	655	2185	0.13
	Acetone	578	699	2995	-
	DMSO	600	711	2003	-

[a] Fluoresce in 1M NaOH (Φ_F = 0.95) was used as the standard in measuring Φ_F for **ABA** and **ABVA**, and cresyl violet in methanol (Φ_F = 0.53) was used as the standard in measuring Φ_F for **AVBVA**.

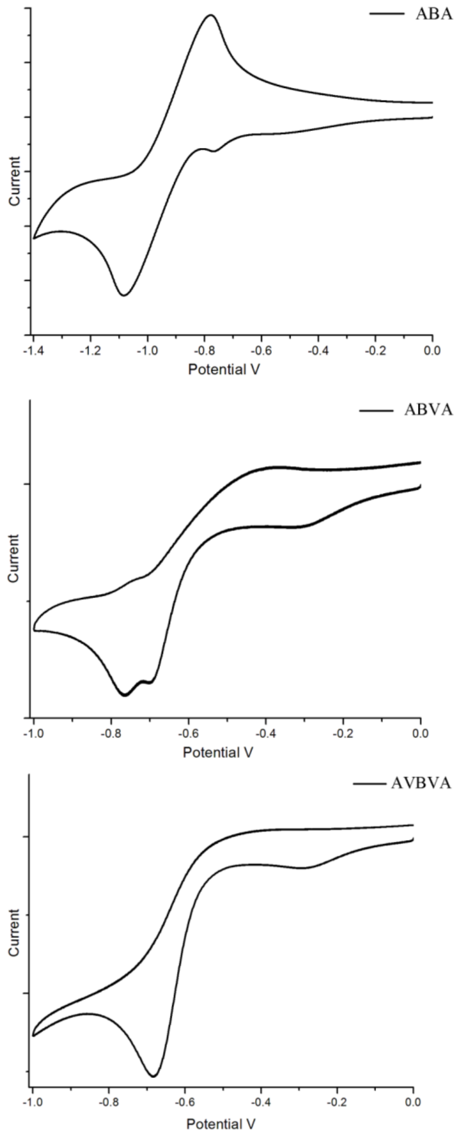

Figure S1. Cyclic voltammetry diagrams of complexes **ABA**, **ABVA** and **AVBVA** in anhydrous CH_2Cl_2 with 0.1 M Bu_4NBF_4 as electrolyte at a scan rate of 50 mV/s.

Figure S2. Pictures of the gels of **ABVA** (left) and **AVBVA** (right) obtained from 1,4-dioxane/cyclohexane (v/v = 1/4).

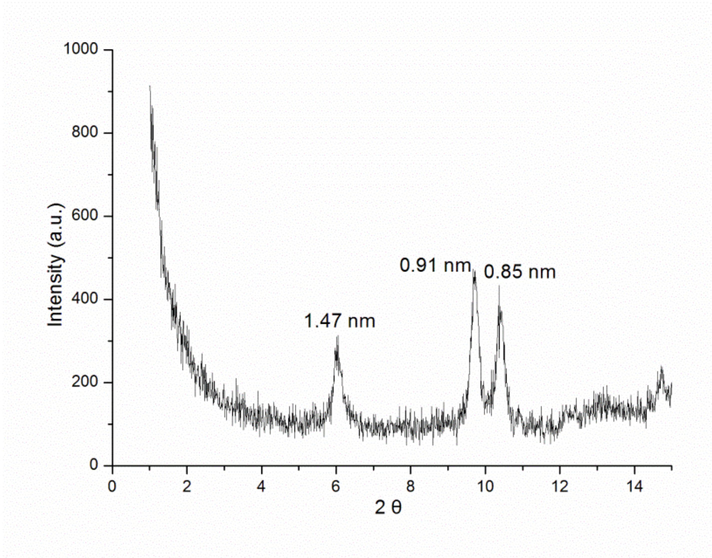

Figure S3. XRD pattern of xerogel **ABVA**.

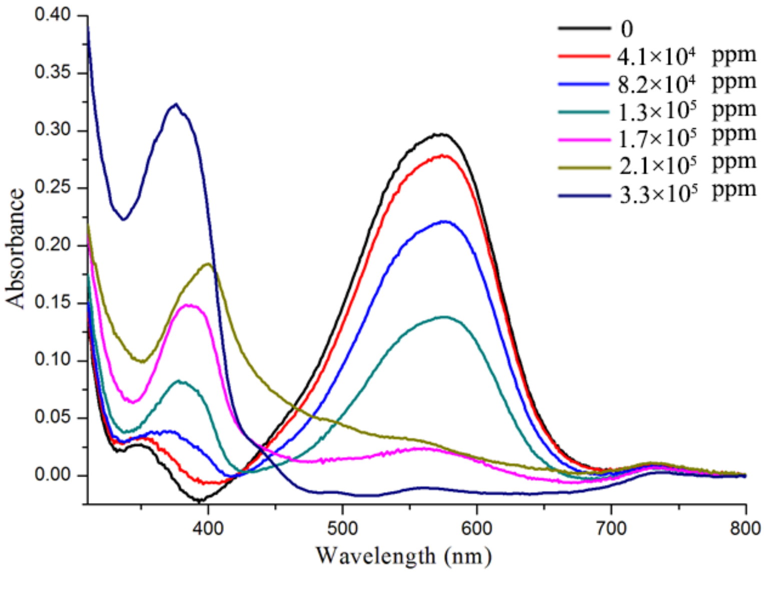

Figure S4. UV-vis absorption spectra of the xerogel-based films of **ABVA** upon exposure to *n*-propylamine in different concentrations for 30 s.

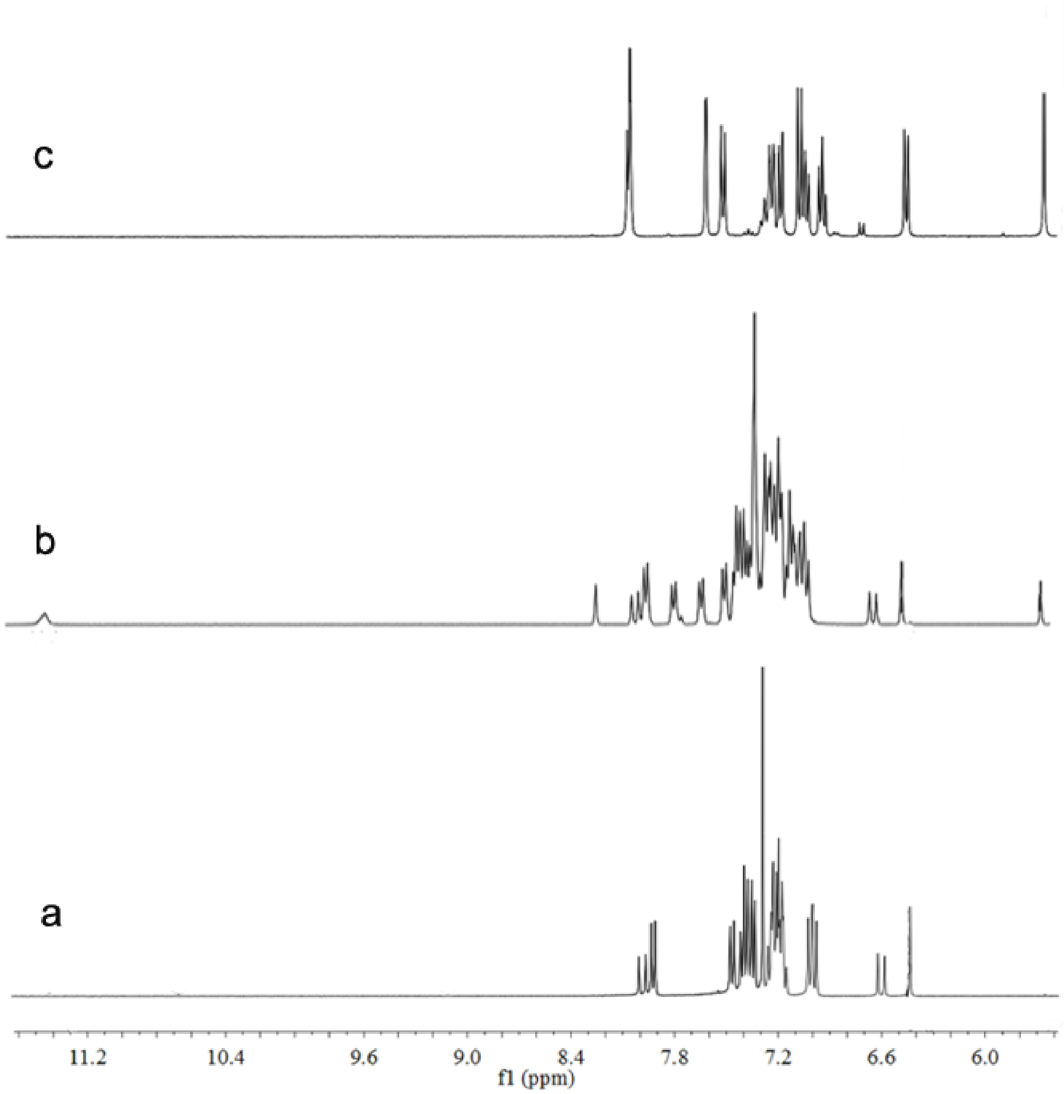

Figure S5. ^{1}H NMR (400 MHz) spectra of **ABVA** in $CDCl_3$ (3.2×10^{-3} M) before (a) and after (b) adding 2.0×10^{3} equiv. of *n*-propylamine as well as (c) further adding a drop of D_2O.

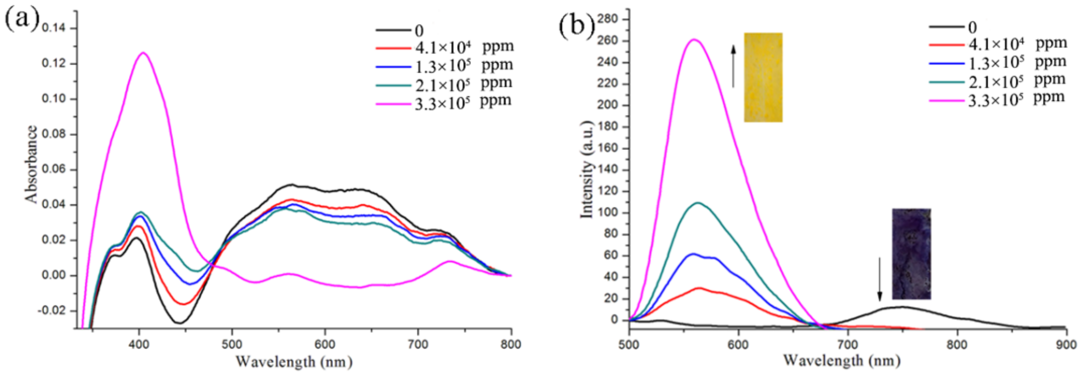

Figure S6. UV-vis absorption (a) and fluorescence emission (b, λ_{ex} = 400 nm) spectra of the xerogel-based film of **AVBVA** upon exposure to *n*-propylamine in different concentrations for 30 s. Insets: the fluorescence enhanced of the xerogel films after being added into a cell filled with the vapors of *n*-propylamine.

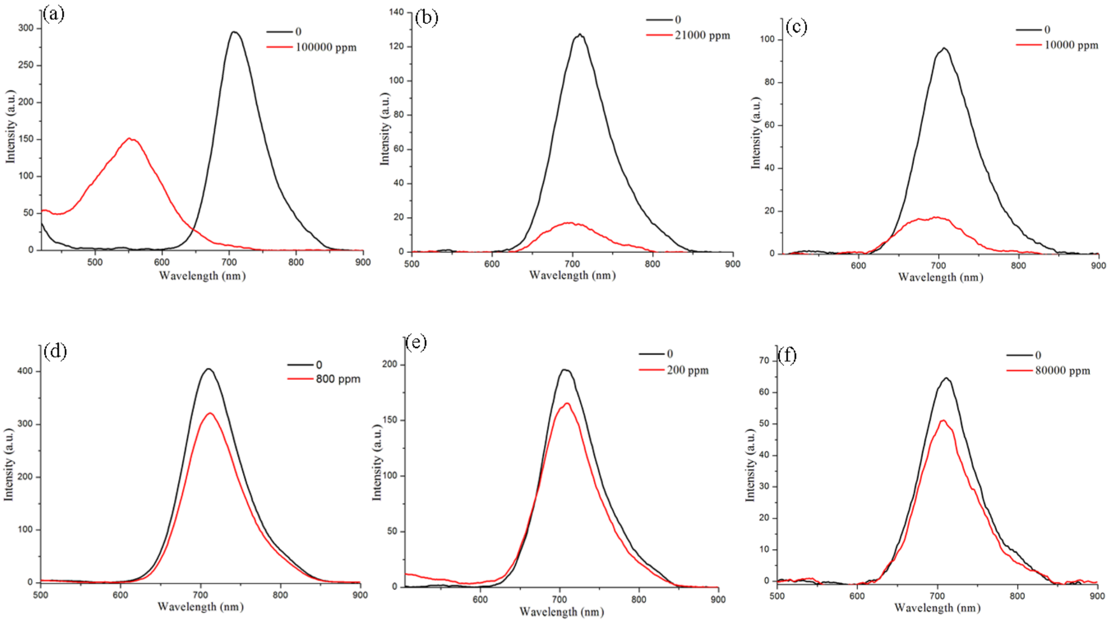

Figure S7. Fluorescence emission spectra of the xerogel film based on **ABVA** upon exposure to saturated vapors of *n*-butylamine (a), pyridine (b), cyclohexylaminein (c), aniline (d), tributylamine (e) and triethylamine (f) for 30 s. The excitation wavelength is 360 nm.

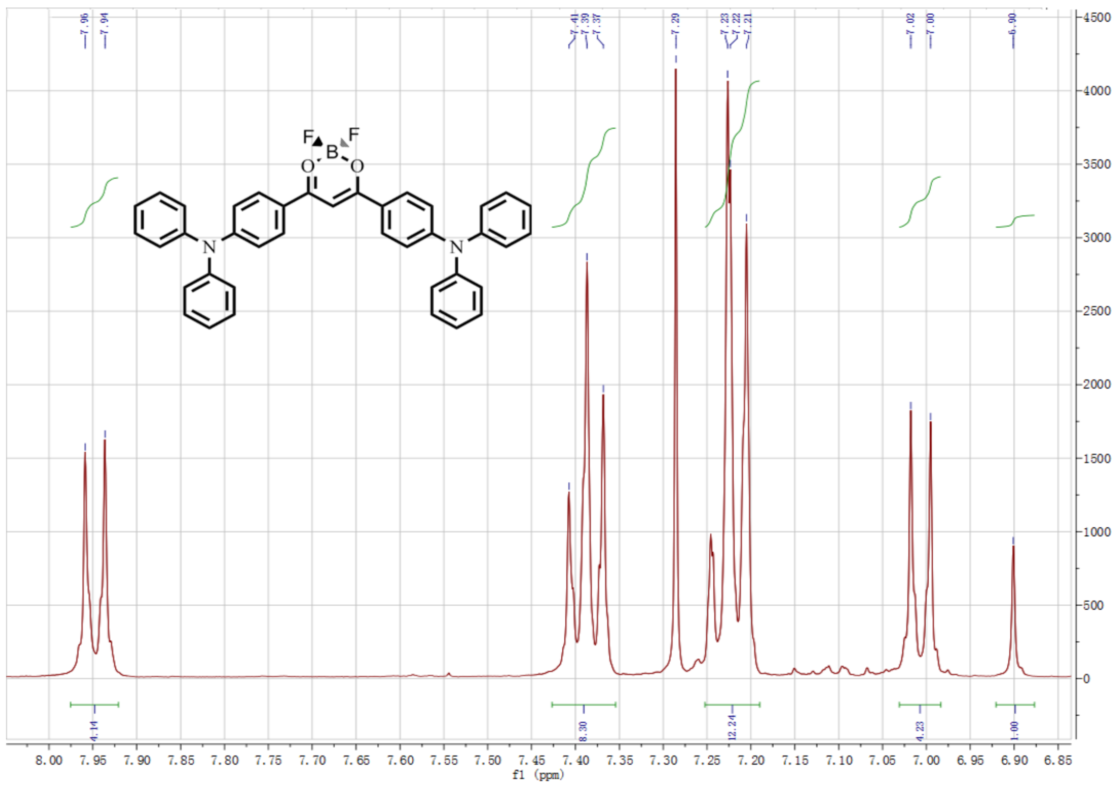

Figure S8. ^{1}H NMR (400 MHz) spectrum of **ABA** in $CDCl_3$.

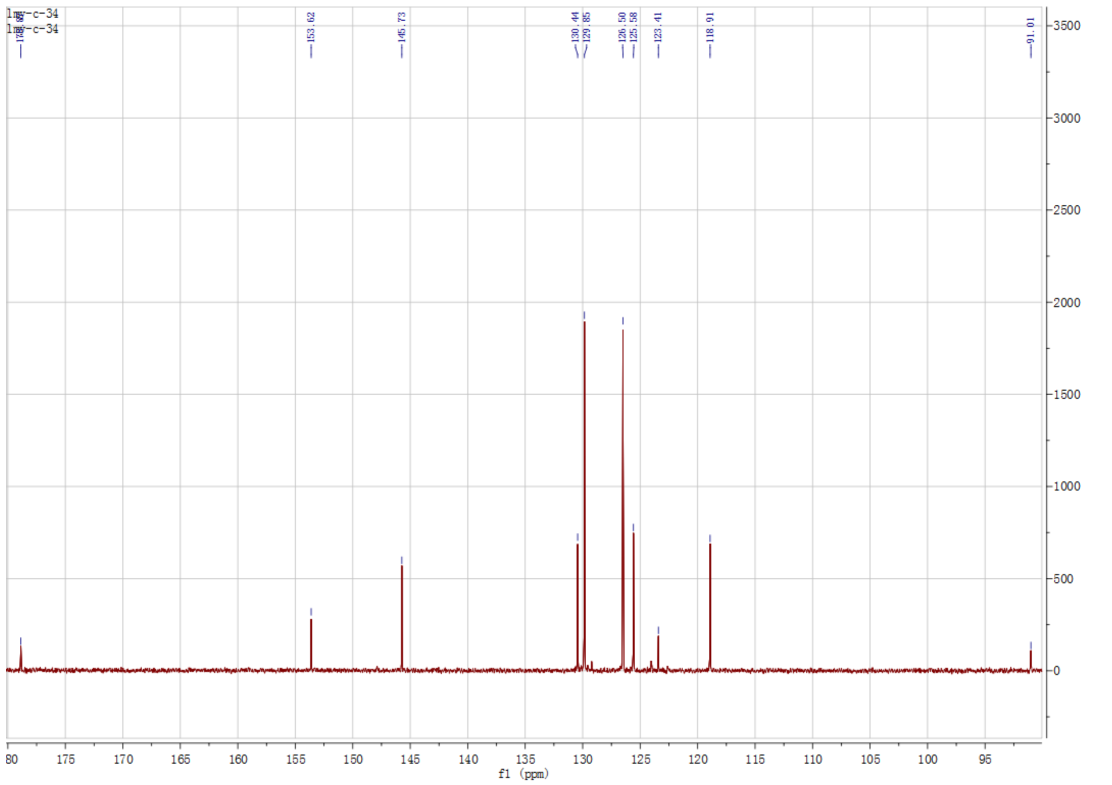

Figure S9. ^{13}C NMR (100 MHz) spectrum of **ABA** in $CDCl_3$.

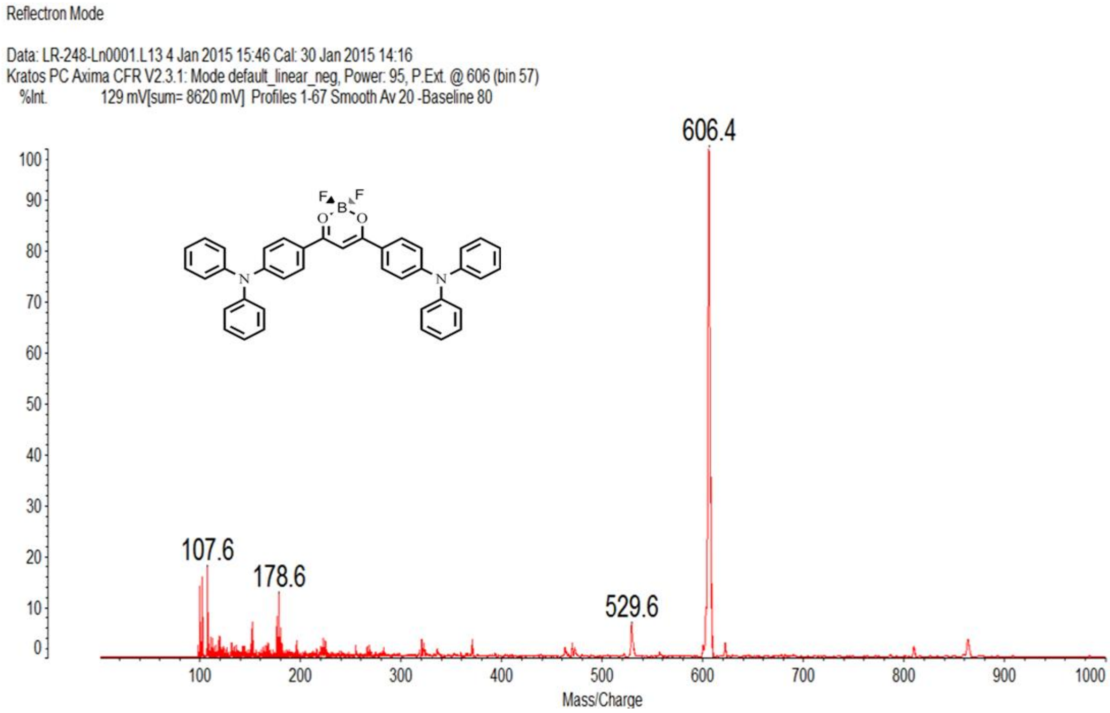

Figure S10. MALDI/TOF MS spectrum of **ABA**.

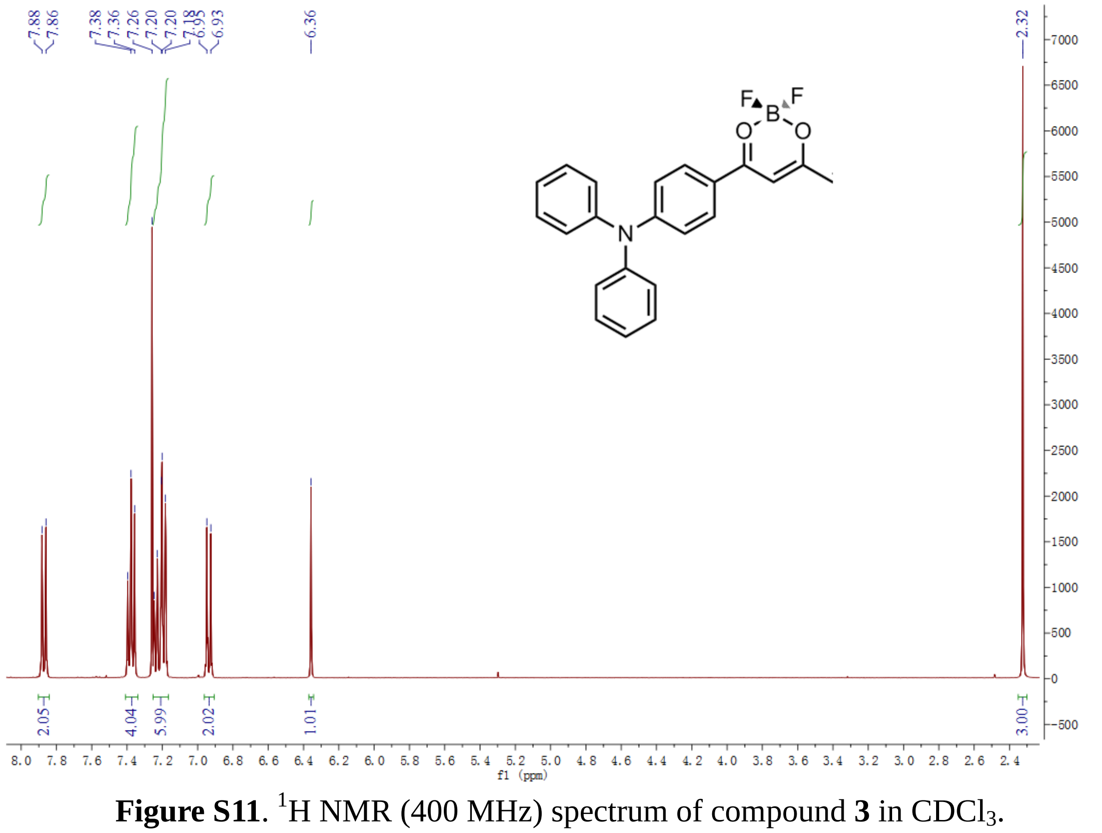

Figure S11. ^{1}H NMR (400 MHz) spectrum of compound **3** in $CDCl_3$.

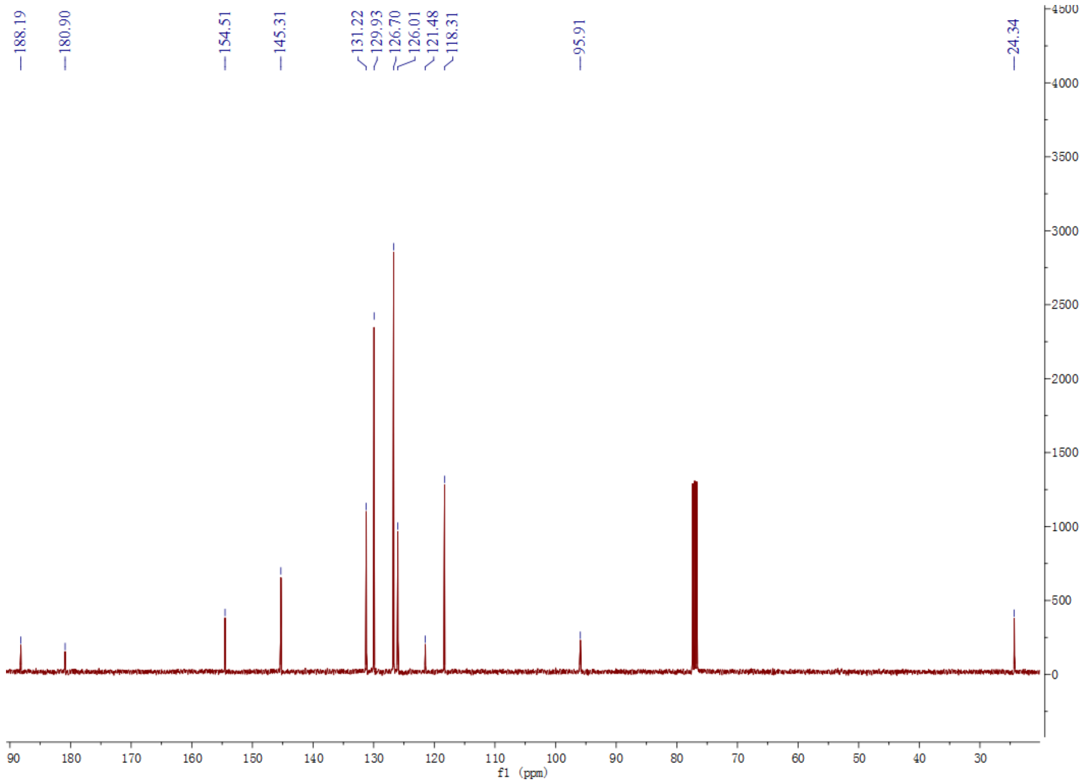

Figure S12. ^{13}C NMR (100 MHz) spectrum of compound **3** in $CDCl_3$.

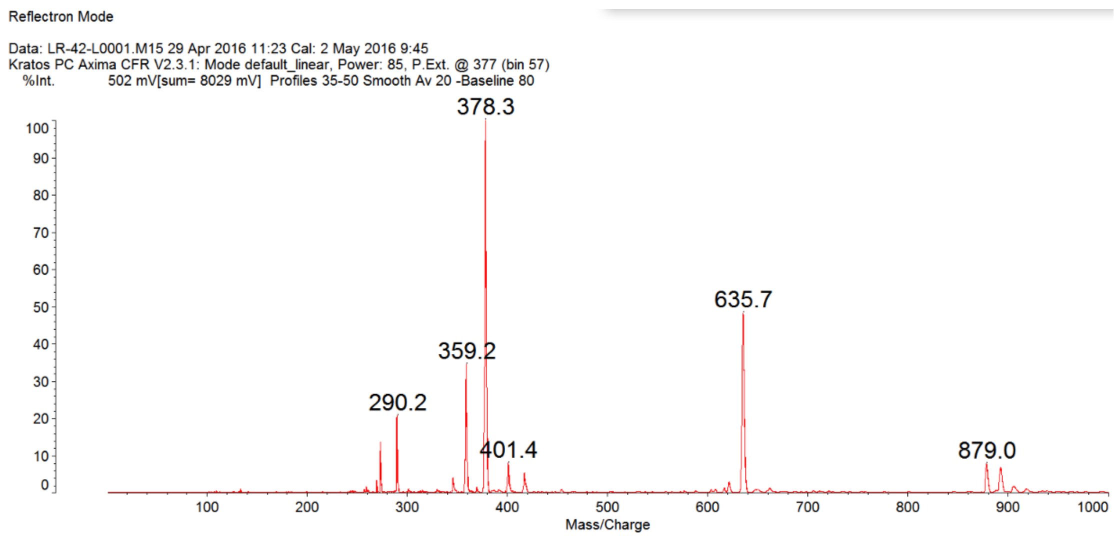

Figure S13. MALDI/TOF MS spectrum of **3**.

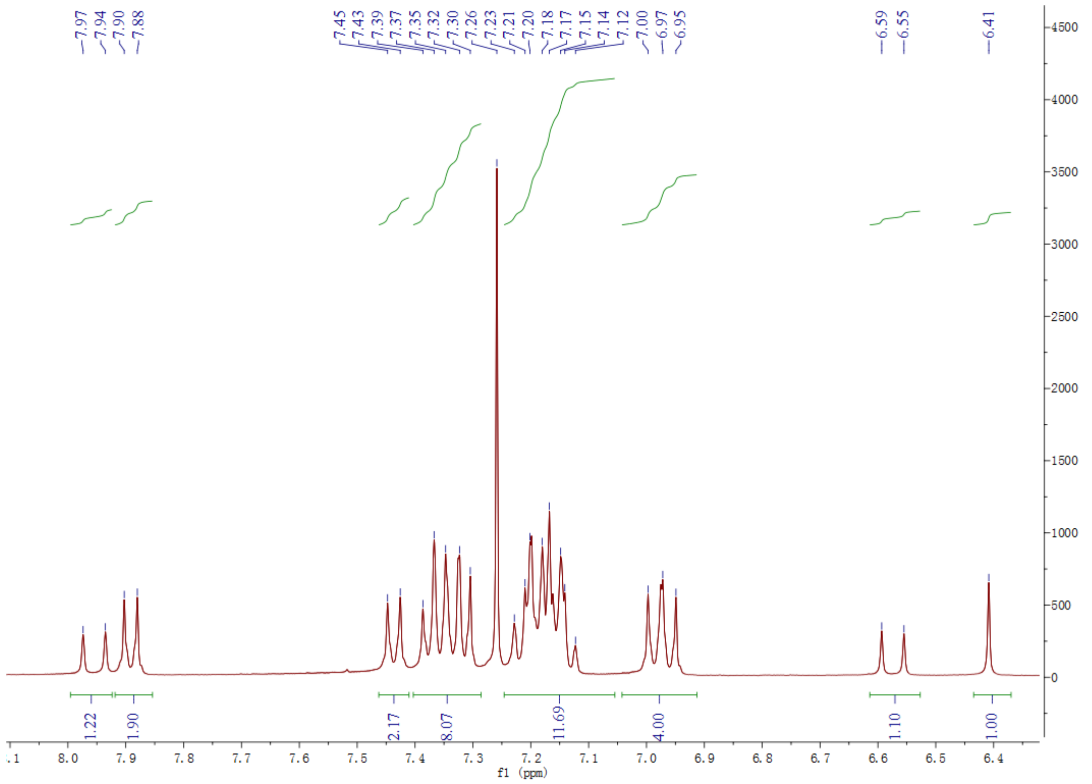

Figure S14. ^{1}H NMR (400 MHz) spectrum of **ABVA** in $CDCl_3$.

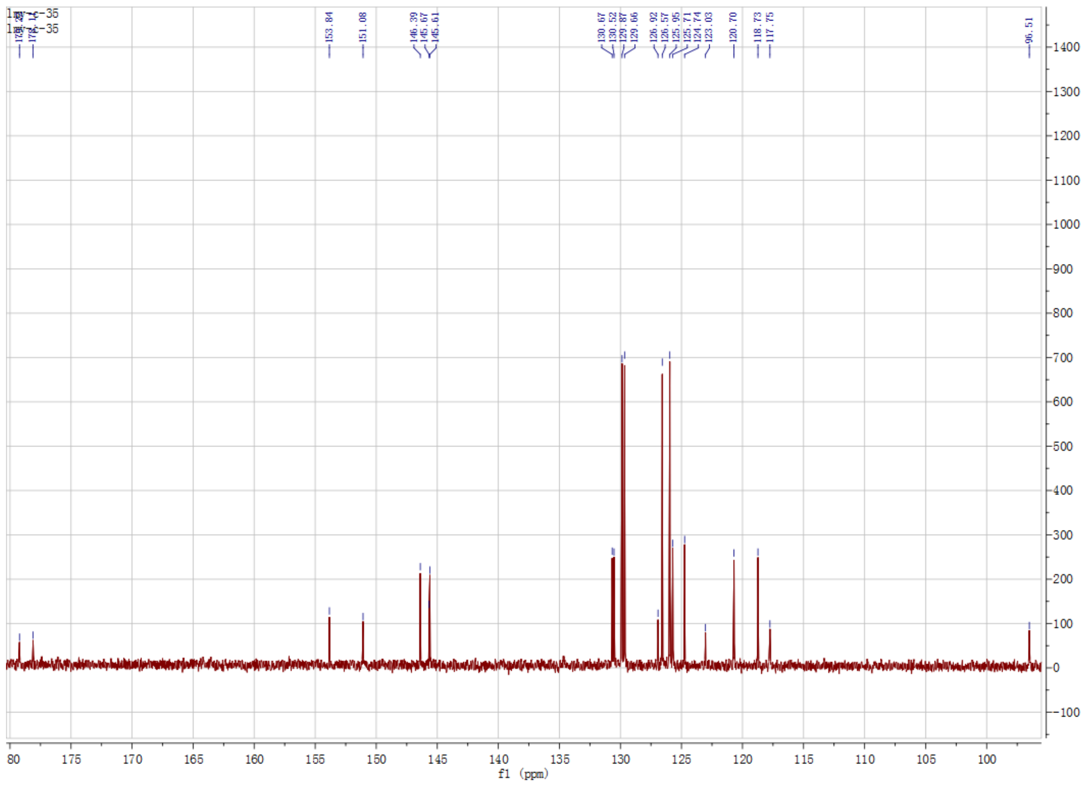

Figure S15. ^{13}C NMR (100 MHz) spectrum of **ABVA** in $CDCl_3$.

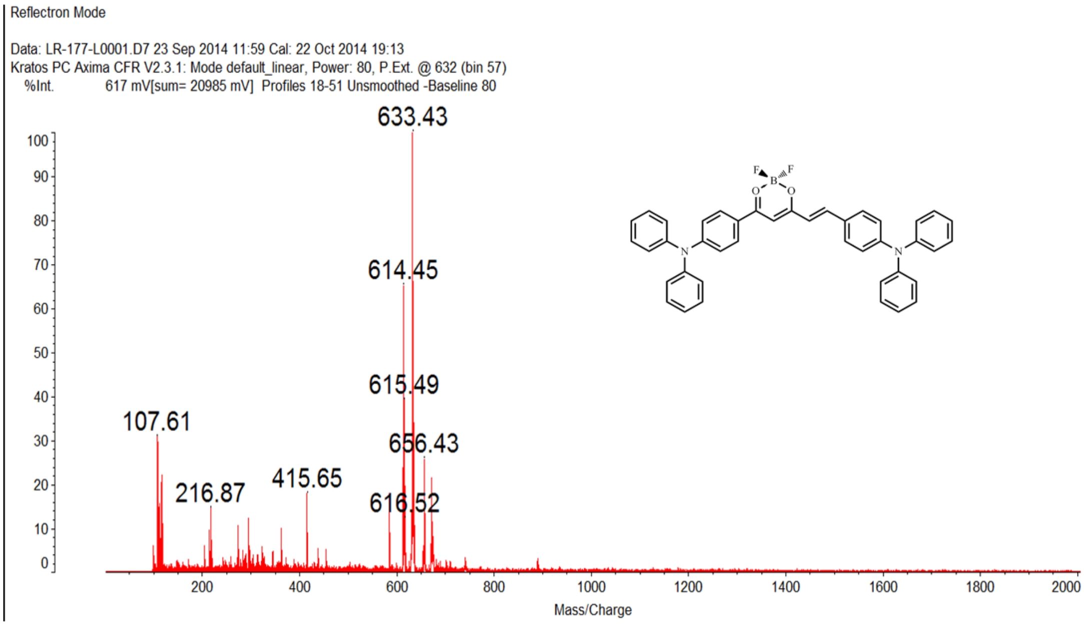

Figure S16. MALDI/TOF MS spectrum of **ABVA**.

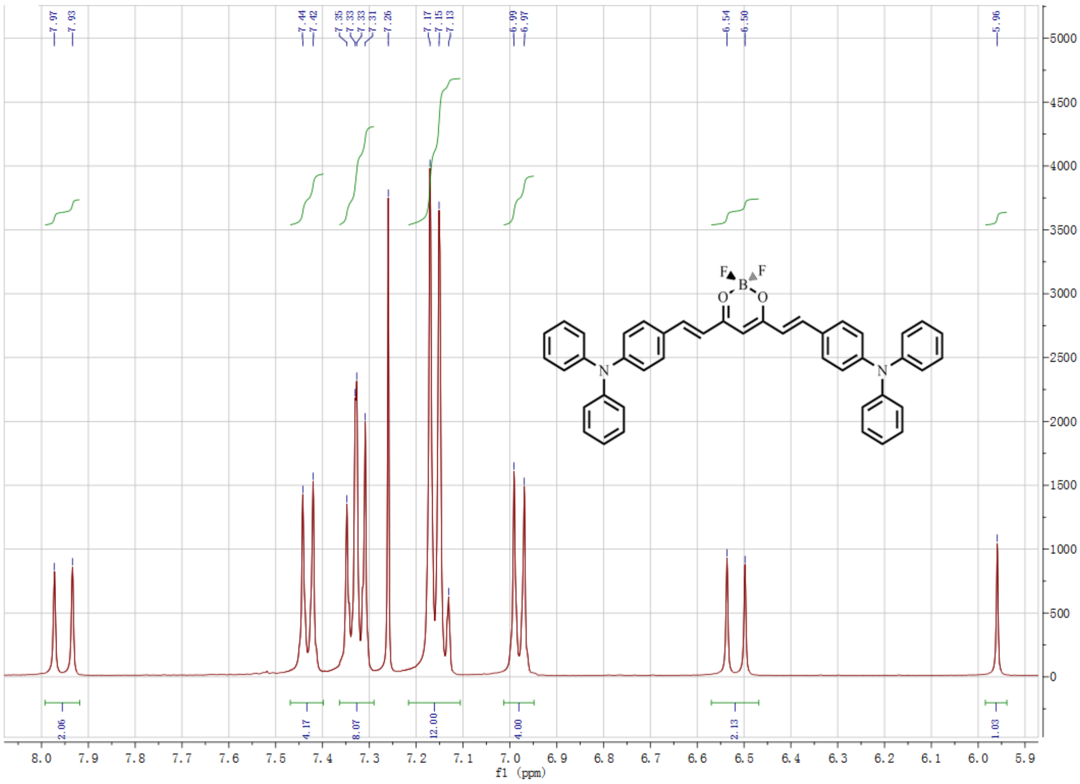

Figure S17. ^{1}H NMR (400 MHz) spectrum of **AVBVA** in $CDCl_3$.

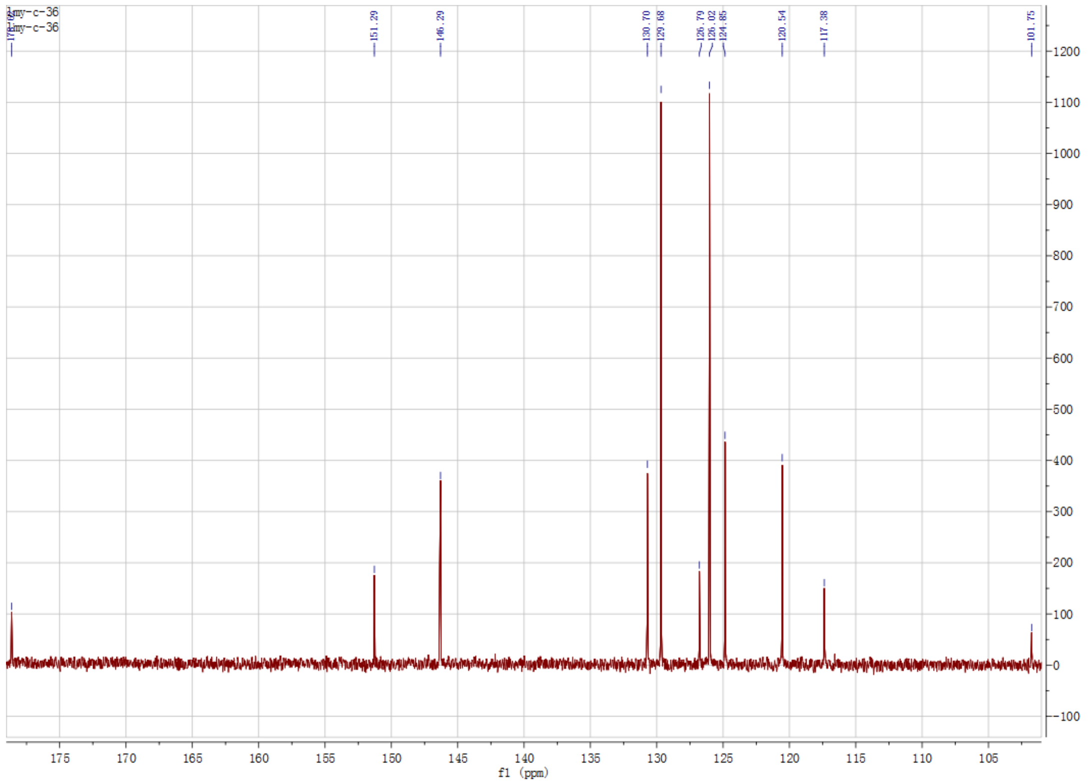

Figure S18. ^{13}C NMR (100 MHz) spectrum of **AVBVA** in $CDCl_3$.

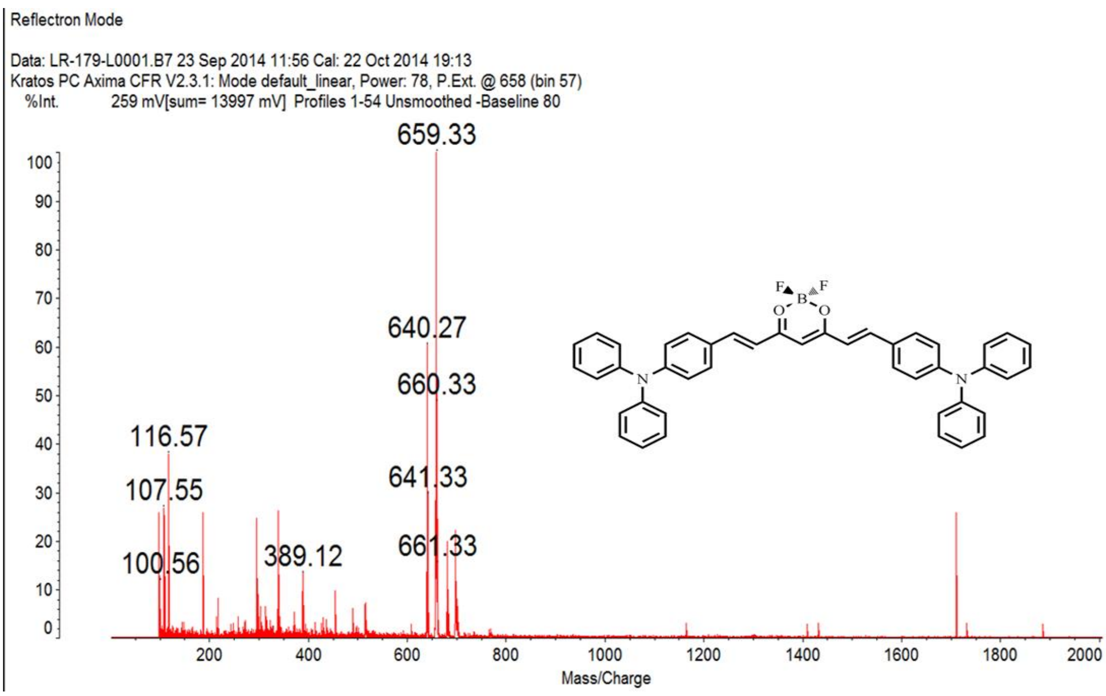

Figure S19. MALDI/TOF MS spectrum of **AVBVA**.